Dirac-like Plasmons in Honeycomb Lattices of Metallic Nanoparticles

Guillaume Weick,[1] Claire Woollacott,[2] William L. Barnes,[2] Ortwin Hess,[3] and Eros Mariani[2]

[1]*Institut de Physique et Chimie des Matériaux de Strasbourg, Université de Strasbourg, CNRS UMR 7504,
23 rue du Loess, BP 43, F-67034 Strasbourg Cedex 2, France*
[2]*Centre for Graphene Science, Department of Physics and Astronomy, University of Exeter,
Stocker Road EX4 4QL Exeter, United Kingdom*
[3]*The Blackett Laboratory, Department of Physics, Imperial College London, South Kensington Campus,
London SW7 2AZ, United Kingdom*

We consider a two-dimensional honeycomb lattice of metallic nanoparticles, each supporting a localized surface plasmon, and study the quantum properties of the collective plasmons resulting from the near-field dipolar interaction between the nanoparticles. We analytically investigate the dispersion, the effective Hamiltonian, and the eigenstates of the collective plasmons for an arbitrary orientation of the individual dipole moments. When the polarization points close to the normal to the plane, the spectrum presents Dirac cones, similar to those present in the electronic band structure of graphene. We derive the effective Dirac Hamiltonian for the collective plasmons and show that the corresponding spinor eigenstates represent Dirac-like massless bosonic excitations that present similar effects to electrons in graphene, such as a nontrivial Berry phase and the absence of backscattering off smooth inhomogeneities. We further discuss how one can manipulate the Dirac points in the Brillouin zone and open a gap in the collective plasmon dispersion by modifying the polarization of the localized surface plasmons, paving the way for a fully tunable plasmonic analogue of graphene.

Light has been the source of inspiration for scientific thinking for millennia. Ancient Assyrians developed the first lenses in order to bend the trajectory of light and control its propagation. In contrast to the macroscopic scale, the use of light to observe microscopic structures poses difficulties due to the diffraction limit [1]. In an attempt to overcome this limit and observe subwavelength structures, plasmonic nanostructures have been created [2,3], such as isolated metallic nanoparticles [4]. The evanescent field at the surface of the nanoparticle, associated with the localized surface plasmon (LSP) resonance [5], produces strong optical field enhancement in the subwavelength region, allowing one to overcome the diffraction limit and achieve resolution at the molecular level [6].

While the field of plasmonics mostly focuses on a single or a few structures, the creation of ordered arrays of nanoparticles constitutes a bridge to the realm of metamaterials. Plasmonic metamaterials exhibit unique properties beyond traditional optics, like a negative refractive index [7], perfect lensing [8], the exciting perspective of electromagnetic invisibility cloaking [9], and "trapped rainbow" slow light exploiting the inherent broadband nature of plasmonics [10]. Indeed, in plasmonic metamaterials, the interaction between LSPs on individual nanoparticles generates extended plasmonic modes involving all LSPs at once [11,12]. Understanding the nature and properties of these plasmonic modes [referred to as "collective plasmons" (CPs) in what follows] is of crucial

importance as they are the channel guiding electromagnetic radiation with strong lateral confinement over macroscopic distances.

CPs in periodic arrays of metallic nanoparticles are an active area of research in plasmonics because the interaction of the LSP resonances can lead to dramatic changes in the overall optical response of such structures. For example, it was both predicted [13] and observed [14] that the plasmonic response of a periodic array of nanoparticles could be significantly narrowed with respect to the single particle response. Further work has shown that these coupled resonances are relevant to applications in light emission [15]. The extended nature of the collective resonances means that there is a scope for harvesting emission from sources spread over large volumes [16,17].

The dispersion of CPs and their physical nature crucially depend on the lattice structure of the metamaterial and on the microscopic interaction between LSPs. A lattice which recently generated remarkable interest in the condensed matter community is the honeycomb structure exhibited by graphene, a two-dimensional (2D) monolayer of carbon atoms [18]. In the case of graphene, the hopping of electrons between neighboring atoms gives rise to a rich band structure characterized by the presence of fermionic massless Dirac quasiparticles close to zero energy [19]. The chirality associated with pseudorelativistic Dirac fermions results in several of the remarkable properties of graphene, such as a nontrivial Berry phase accumulated in parallel transport [20] and the suppression of electronic backscattering from

smooth scatterers [21]. Undoubtedly, it would be exciting to harvest the remarkable physical properties of electrons in graphene in suitably designed plasmonic metamaterials by analyzing the Hamiltonian and the consequent nature of CP eigenmodes in 2D honeycomb lattices of metallic nanoparticles. This is the purpose of the present theoretical Letter.

We analytically show how the problem of interacting LSPs in the honeycomb structure can be mapped onto the kinetic problem of electrons hopping in graphene, yielding massless Dirac-like bosonic CPs in the vicinity of two Dirac points in the Brillouin zone. The conical dispersion of classical plasmons in a honeycomb lattice of nanoparticles has been discussed numerically in the past for out-of-plane or purely in-plane polarizations [22]. In quite different physical systems (e.g., photonic crystals [23], acoustic waves in periodic hole arrays [24], or cold atoms [25]), conical dispersions were also found in "artificial graphene" due to the honeycomb symmetry. However, the existence of a conical dispersion is not sufficient [26] to prove the physical analogy between quantum CPs in honeycomb plasmonic lattices and electrons in graphene. In order to achieve that, here we unveil the *full Dirac Hamiltonian* of quantum CPs as well as the pseudospin structure of the CP eigenmodes for dipolar LSPs with *arbitrary* orientation. The existence of Dirac points is robust for a small in-plane component of the polarization, where the system maps to strained graphene [27], while band gaps can emerge for increasing in-plane polarization. At energies away from the Dirac point, van Hove singularities emerge in the CP density of states (DOS), associated with Lifshitz transitions in the topology of equipotential lines [28]. Our analysis highlights the physical nature of CP eigenmodes as well as the tunability of their band structure and of the corresponding DOS with the polarization of light, which can be crucial for enhancing the coupling of light with the plasmonic metamaterial at different wavelengths.

Specifically, we consider an ensemble of identical spherical metallic nanoparticles of radius r forming a 2D honeycomb lattice with lattice constant a embedded in a dielectric medium with dielectric constant ϵ_m (see Fig. 1). The nanoparticles are located at positions $\mathbf{R}_s$, with $s = A$, B a sublattice index which distinguishes the inequivalent lattice sites. Each individual nanoparticle supports an LSP resonance which can be triggered by an oscillating external electric field with wavelength λ much larger than r. Under such a condition, the LSP is a dipolar collective electronic excitation at the Mie frequency $\omega_0 = \omega_p/\sqrt{1 + 2\epsilon_m}$, which typically lies in the visible or near-infrared part of the spectrum [5]. Here, $\omega_p = \sqrt{4\pi n_e e^2/m_e}$ is the plasma frequency, with n_e, $-e$, and m_e the electron density, charge, and mass, respectively. The LSP corresponding to the electronic center-of-mass excitation can be generally considered as a quantum bosonic mode, particularly when the size of the nanoparticle is such that quantization effects are important [29–32]. The noninteracting part of the
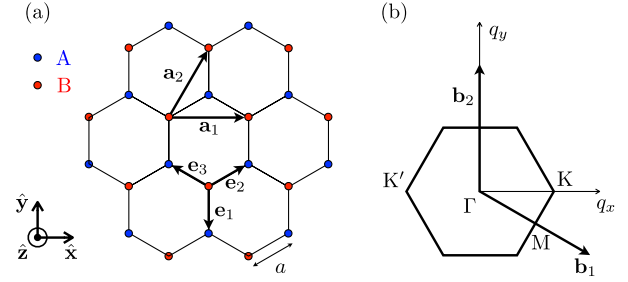

FIG. 1 (color online). (a) Honeycomb lattice with lattice constant a and lattice vectors $\mathbf{a}_1 = a(\sqrt{3}, 0)$ and $\mathbf{a}_2 = a(\frac{\sqrt{3}}{2}, \frac{3}{2})$. The three vectors $\mathbf{e}_1 = a(0, -1)$, $\mathbf{e}_2 = a(\frac{\sqrt{3}}{2}, \frac{1}{2})$, and $\mathbf{e}_3 = a(-\frac{\sqrt{3}}{2}, \frac{1}{2})$ connect the A and B inequivalent lattice sites [dark gray (blue) and light gray (red) dots in the figure]. (b) First Brillouin zone in reciprocal space with primitive vectors $\mathbf{b}_1 = \frac{2\pi}{3a}(\sqrt{3}, -1)$ and $\mathbf{b}_2 = \frac{4\pi}{3a}(0, 1)$.

Hamiltonian describing the independent LSPs on the honeycomb lattice sites reads $H_0 = \sum_{s=A,B} \sum_{\mathbf{R}_s} [\Pi_s^2(\mathbf{R}_s)/2M + M\omega_0^2 h_s^2(\mathbf{R}_s)/2]$, where $h_s(\mathbf{R})$ is the displacement field associated with the electronic center of mass at position $\mathbf{R}$, $\Pi_s(\mathbf{R})$ its conjugated momentum, and $M = N_e m_e$ its mass, with N_e the number of valence electrons in each nanoparticle [30,31].

The nature of the coupling between LSPs in different nanoparticles depends on their size and distance. Provided that the wavelength associated with each LSP is much larger than the interparticle distance a and that $r \lesssim a/3$ [12], each LSP can be considered as a point dipole with dipole moment $\mathbf{p} = -eN_e h_s(\mathbf{R})\hat{\mathbf{p}}$ which interacts with the neighboring ones through dipole-dipole interaction. Moreover, it has been numerically shown [22] that a quasistatic approximation which only takes into account the near field generated by each dipole qualitatively reproduces the results of more sophisticated simulations in which retardation effects are included. Within such a quasistatic approximation, the interaction between two dipoles $\mathbf{p}$ and $\mathbf{p}'$ located at $\mathbf{R}$ and $\mathbf{R}'$, respectively, reads $\mathcal{V} = [\mathbf{p} \cdot \mathbf{p}' - 3(\mathbf{p} \cdot \mathbf{n})(\mathbf{p}' \cdot \mathbf{n})]/\epsilon_m|\mathbf{R} - \mathbf{R}'|^3$, with $\mathbf{n} = (\mathbf{R} - \mathbf{R}')/|\mathbf{R} - \mathbf{R}'|$ [33]. In what follows, we assume that in a CP eigenmode all nanoparticles are polarized in the same direction $\hat{\mathbf{p}} = \sin\theta(\sin\varphi\hat{\mathbf{x}} - \cos\varphi\hat{\mathbf{y}}) + \cos\theta\hat{\mathbf{z}}$, where θ is the angle between $\hat{\mathbf{p}}$ and $\hat{\mathbf{z}}$ and φ is the angle between the projection of $\hat{\mathbf{p}}$ in the xy plane and $\mathbf{e}_1$ [see Fig. 1(a)]. This can be achieved by an external electric field associated with light of suitable polarization. We thus write the total Hamiltonian of our system of coupled LSPs as $H = H_0 + H_{\text{int}}$, where the dipole-dipole interaction term reads

$$H_{\text{int}} = \frac{(eN_e)^2}{\epsilon_m a^3} \sum_{\mathbf{R}_B} \sum_{j=1}^{3} \mathcal{C}_j h_B(\mathbf{R}_B) h_A(\mathbf{R}_B + \mathbf{e}_j). \quad (1)$$

Here, $\mathcal{C}_j = 1 - 3\sin^2\theta\cos^2(\varphi - 2\pi[j-1]/3)$, and the vectors $\mathbf{e}_j$ connect the A and B sublattices [see Fig. 1(a)]. In Eq. (1), we only consider the dipole-dipole interaction

between nearest neighbors, as the effect of interactions beyond nearest neighbors does not qualitatively change the plasmonic spectrum [34].

The analogy between the plasmonic structure of Fig. 1 and the electronic properties of graphene becomes transparent by introducing the bosonic ladder operators $a_{\mathbf{R}}|b_{\mathbf{R}} = (M\omega_0/2\hbar)^{1/2}h_{A|B}(\mathbf{R}) + i\Pi_{A|B}(\mathbf{R})/(2\hbar M\omega_0)^{1/2}$ which satisfy the commutation relations $[a_{\mathbf{R}}, a_{\mathbf{R}'}^{\dagger}] = [b_{\mathbf{R}}, b_{\mathbf{R}'}^{\dagger}] = \delta_{\mathbf{R},\mathbf{R}'}$ and $[a_{\mathbf{R}}, b_{\mathbf{R}'}^{\dagger}] = 0$. As we will show in the following, the introduction of such operators not only gives access to the plasmon dispersion (which can be calculated classically as well [34]) but also unveils the Dirac nature of the CP quantum states. The harmonic Hamiltonian H_0 can be written in terms of the abovementioned bosonic operators as $H_0 = \hbar\omega_0\sum_{\mathbf{R}_A} a_{\mathbf{R}_A}^{\dagger} a_{\mathbf{R}_A} + \hbar\omega_0\sum_{\mathbf{R}_B} b_{\mathbf{R}_B}^{\dagger} b_{\mathbf{R}_B}$, while Eq. (1) transforms into

$$H_{\text{int}} = \hbar\Omega\sum_{\mathbf{R}_B}\sum_{j=1}^{3}\mathcal{C}_j b_{\mathbf{R}_B}^{\dagger}(a_{\mathbf{R}_B+\mathbf{e}_j} + a_{\mathbf{R}_B+\mathbf{e}_j}^{\dagger}) + \text{H.c.} \quad (2)$$

In Eq. (2), $\Omega = \omega_0(r/a)^3(1 + 2\epsilon_m)/6\epsilon_m$, such that $\Omega \ll \omega_0$. The first term on the right-hand side of Eq. (2) resembles the electronic tight-binding Hamiltonian of graphene [19], except for three major differences. (i) The Hamiltonian of graphene describes fermionic particles (electrons), while we deal here with *bosonic* excitations (LSPs). (ii) In graphene, an electron "hops" from one lattice site to a neighboring one; i.e., the underlying mechanism linking the two inequivalent sublattices is purely kinetic. In the present case, the mechanism coupling the two sublattices is purely induced by near-field (dipolar) *interactions*, leading to the creation of an LSP excitation at lattice site $\mathbf{R}_B$ and the annihilation of another LSP at a nearest neighbor located at $\mathbf{R}_B + \mathbf{e}_j$. (iii) In (unstrained) graphene, the hopping matrix element between two neighboring atoms is the same for all three bonds. In contrast, in our case, the three energy scales $\hbar\Omega\mathcal{C}_j$ in Eq. (1) are in general different and can be tuned by the direction of the polarization $\hat{\mathbf{p}}$ of the CP eigenmode, which can be controlled by means of an external light field. For $0 < \theta \leq \theta_0$ and $\pi - \theta_0 \leq \theta < \pi$ with $\theta_0 = \arcsin\sqrt{1/3}$, the coefficients $\mathcal{C}_j$ are all positive for any φ and have different values, resulting in different couplings between the bonds and thus mimicking the effect of strain in the lattice [27]. For $\theta_0 < \theta < \pi - \theta_0$, the signs of the coefficients $\mathcal{C}_j$ depend on φ, and the analogy with strained graphene is no longer valid. In the special case where $\mathcal{C}_1 = \mathcal{C}_2 = \mathcal{C}_3$ (for $\theta = 0$ or π), we expect the CP spectrum to resemble that of the electronic band structure in graphene since the Bloch theorem does not depend on the quantum statistics of the particles one considers but only on the structure of the periodic lattice. This fact is also responsible for the conical dispersion presented by other systems with honeycomb symmetry [23–25]. As we will now show, two slight

differences appear in the CP dispersion as compared to the graphene band structure; i.e., the effect of the Hamiltonian H_0 is to produce a global energy shift (by an amount $\hbar\omega_0$), while the "anomalous" term $\propto b_{\mathbf{R}_B}^{\dagger} a_{\mathbf{R}_B+\mathbf{e}_j}^{\dagger}$ in Eq. (2) introduces corrections of order $(\Omega/\omega_0)^2$ to the spectrum.

Introducing the bosonic operators in momentum space $a_{\mathbf{q}}$ and $b_{\mathbf{q}}$ through $a_{\mathbf{R}}|b_{\mathbf{R}} = \mathcal{N}^{-1/2}\sum_{\mathbf{q}}\exp(i\mathbf{q}\cdot\mathbf{R})a_{\mathbf{q}}|b_{\mathbf{q}}$, with $\mathcal{N}$ the number of unit cells of the honeycomb lattice, the Hamiltonian $H = H_0 + H_{\text{int}}$ transforms into $H = \hbar\omega_0\sum_{\mathbf{q}}(a_{\mathbf{q}}^{\dagger} a_{\mathbf{q}} + b_{\mathbf{q}}^{\dagger} b_{\mathbf{q}}) + \hbar\Omega\sum_{\mathbf{q}}[f_{\mathbf{q}} b_{\mathbf{q}}^{\dagger}(a_{\mathbf{q}} + a_{-\mathbf{q}}^{\dagger}) + \text{H.c.}]$, with $f_{\mathbf{q}} = \sum_{j=1}^{3}\mathcal{C}_j\exp(i\mathbf{q}\cdot\mathbf{e}_j)$. The latter Hamiltonian is diagonalized by two successive Bogoliubov transformations. First, we introduce the two bosonic operators $\alpha_{\mathbf{q}}^{\pm} = [(f_{\mathbf{q}}/|f_{\mathbf{q}}|)a_{\mathbf{q}} \pm b_{\mathbf{q}}]/\sqrt{2}$ in terms of which we obtain $H = \sum_{\tau=\pm}\sum_{\mathbf{q}}[(\hbar\omega_0 + \tau\hbar\Omega|f_{\mathbf{q}}|)\alpha_{\mathbf{q}}^{\tau\dagger}\alpha_{\mathbf{q}}^{\tau} + \tau\frac{\hbar\Omega|f_{\mathbf{q}}|}{2} \times (\alpha_{\mathbf{q}}^{\tau\dagger}\alpha_{-\mathbf{q}}^{\tau\dagger} + \text{H.c.})]$. Second, we define two new bosonic modes $\beta_{\mathbf{q}}^{\pm} = \cosh\vartheta_{\mathbf{q}}^{\pm}\alpha_{\mathbf{q}}^{\pm} - \sinh\vartheta_{\mathbf{q}}^{\pm}\alpha_{-\mathbf{q}}^{\pm\dagger}$, with $\cosh\vartheta_{\mathbf{q}}^{\pm} = 2^{-1/2}[(1 \pm \Omega|f_{\mathbf{q}}|/\omega_0)/(1 \pm 2\Omega|f_{\mathbf{q}}|/\omega_0)^{1/2} + 1]^{1/2}$ and $\sinh\vartheta_{\mathbf{q}}^{\pm} = \mp 2^{-1/2}[(1 \pm \Omega|f_{\mathbf{q}}|/\omega_0)/(1 \pm 2\Omega|f_{\mathbf{q}}|/\omega_0)^{1/2} - 1]^{1/2}$, which diagonalize the Hamiltonian H as

$$H = \sum_{\tau=\pm}\sum_{\mathbf{q}}\hbar\omega_{\mathbf{q}}^{\tau}\beta_{\mathbf{q}}^{\tau\dagger}\beta_{\mathbf{q}}^{\tau}, \qquad \omega_{\mathbf{q}}^{\pm} = \omega_0\sqrt{1 \pm 2\frac{\Omega}{\omega_0}|f_{\mathbf{q}}|}.$$
$$(3)$$

The two CP branches reduce to $\omega_{\mathbf{q}}^{\pm} \simeq \omega_0 \pm \Omega|f_{\mathbf{q}}|$ to first order in $\Omega/\omega_0 \ll 1$, for which we have $\beta_{\mathbf{q}}^{\pm} \simeq \alpha_{\mathbf{q}}^{\pm}$ [34].

The dispersion in Eq. (3) is shown in Fig. 2 in the case of a polarization $\hat{\mathbf{p}}$ perpendicular to the plane of the honeycomb lattice [$\theta = 0$, Fig. 2(a)], in the case of an in-plane polarization [$\theta = \pi/2$, $\varphi = 0$, Fig. 2(b)], and for the special case $\theta = \arcsin\sqrt{1/3}$, $\varphi = 0$ [Fig. 2(c)]. In the first case [Fig. 2(a)], we have gapless modes with two inequivalent Dirac cones centered at the K and K' points located at $\pm\mathbf{K} = \frac{4\pi}{3\sqrt{3}a}(\pm 1, 0)$ in the first Brillouin zone [cf. Fig. 1(b)], while, in the second case, the modes are gapped [Fig. 2(b)]. The dispersion shown in Fig. 2(c) corresponds to a polarization for which $\mathcal{C}_1 = 0$ in Eq. (1); i.e., the bonds linked by $\mathbf{e}_1$ [cf. Fig. 1(a)] are ineffective and the system is effectively translationally invariant along one direction. Hence, the CP dispersion in Fig. 2(c) does not depend on q_y and presents Dirac "lines."

The analogy between the dispersion shown in Fig. 2(a) and the electronic band structure of graphene [19] is striking. Close to the two inequivalent Dirac points K and K' [see Fig. 1(b)], the function $f_{\mathbf{q}}$ expands as $f_{\mathbf{q}} \simeq -\frac{3a}{2} \times (\pm k_x + ik_y)$, with $\mathbf{q} = \pm\mathbf{K} + \mathbf{k}$ ($|\mathbf{k}| \ll |\mathbf{K}|$), such that the dispersion in Eq. (3) is linear and forms a Dirac cone $\omega_{\mathbf{k}}^{\pm} \simeq \omega_0 \pm v|\mathbf{k}|$, with group velocity $v = 3\Omega a/2$. This feature is consistent with numerical analysis [22]. Moreover, by expanding Eq. (3) in the vicinity of the Dirac points, we can identify the Hamiltonian $H^{\text{eff}} = \sum_{\mathbf{k}}\hat{\Psi}_{\mathbf{k}}^{\dagger}\mathcal{H}_{\mathbf{k}}^{\text{eff}}\hat{\Psi}_{\mathbf{k}}$ that
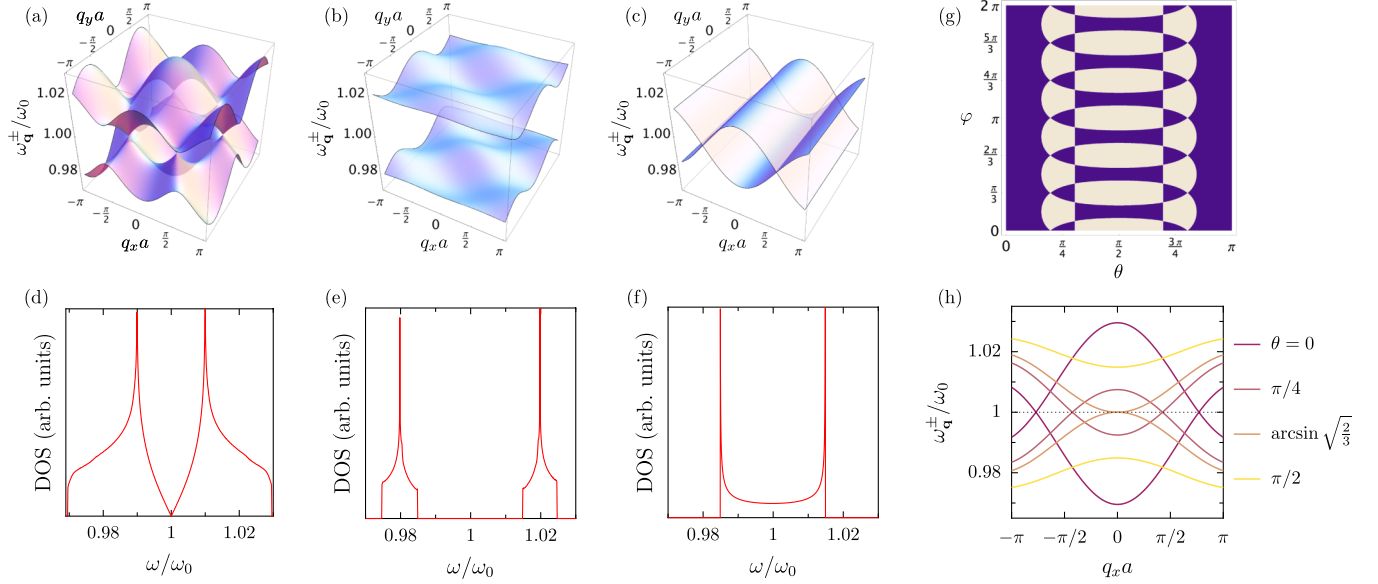
FIG. 2 (color online).   (a)–(c) Collective plasmon dispersion relation from Eq. (3) and (d)–(f) corresponding density of states for (a),
(d) the out-of-plane mode ($\theta = 0$), (b), (e) one in-plane mode ($\theta = \pi/2$), and (c), (f) $\theta = \arcsin\sqrt{1/3}$. (g) Polarization angles (θ, φ)
for which the collective plasmon dispersion is gapless (dark blue regions) and gapped (white regions). (h) Collective plasmon
dispersion along the $K'\Gamma K$ direction ($q_y = 0$) for different orientations θ of the dipoles. In the figure, $\varphi = 0$ and $\Omega/\omega_0 = 0.01$.

effectively describes the CPs. Here, $\hat{\Psi}_{\mathbf{k}} = (a_{\mathbf{k},K}, b_{\mathbf{k},K}, b_{\mathbf{k},K'}, a_{\mathbf{k},K'})$ is a spinor operator, where K and K' denote the valley indices associated with the inequivalent Dirac points, and the 4×4 Hamiltonian reads

$$\mathcal{H}_{\mathbf{k}}^{\text{eff}} = \hbar\omega_0\mathbb{1} - \hbar v\tau_z \otimes \boldsymbol{\sigma} \cdot \mathbf{k}. \qquad (4)$$

In this notation, $\mathbb{1}$ corresponds to the identity matrix, τ_z to the Pauli matrix acting on the valley space (K/K'), while $\boldsymbol{\sigma} = (\sigma_x, \sigma_y)$ is the vector of Pauli matrices acting on the sublattice space (A/B). Up to a global energy shift of $\hbar\omega_0$, Eq. (4) corresponds to a *massless Dirac Hamiltonian* that is fulfilled by CPs, in complete analogy with electrons in graphene [19]. The CP eigenstates of Eq. (4), $\psi_{\mathbf{k},K}^{\pm} = \frac{1}{\sqrt{2}} \times (1, \mp e^{i\xi_{\mathbf{k}}}, 0, 0)$ and $\psi_{\mathbf{k},K'}^{\pm} = \frac{1}{\sqrt{2}}(0, 0, 1, \pm e^{i\xi_{\mathbf{k}}})$ with $\xi_{\mathbf{k}} = \arctan(k_y/k_x)$, are characterized by chirality $\boldsymbol{\sigma} \cdot \hat{\mathbf{k}} = \pm 1$. As a consequence, CPs will show similar effects to electrons in graphene, such as a Berry phase of π [20] and the absence of backscattering off smooth inhomogeneities [21]. This could have crucial implications for the efficient plasmonic propagation in array-based metamaterials.

In Figs. 2(d)–2(f), we show the DOS corresponding to the spectrum illustrated in Figs. 2(a)–2(c). It is interesting to notice the tunability of the DOS with the direction of the polarization, as well as the emergence of van Hove singularities. The latter are associated with Lifshitz transitions [28] in the topology of equipotential lines that percolate at specific energies. The tunability of van Hove singularities in the spectrum could be of crucial importance to increase the coupling of light of different wavelengths with extended CP modes.

For an arbitrary polarization of the LSPs, we can determine if the CP dispersion is gapless by imposing $|f_{\mathbf{q}}| = 0$ in Eq. (3), which leads to the condition $0 \leq [(\mathcal{C}_2 + \mathcal{C}_3)^2 - \mathcal{C}_1^2]/4\mathcal{C}_2\mathcal{C}_3 \leq 1$ for having gapless plasmonic modes [34]. In Fig. 2(g), we show in dark blue the regions of stability of a massless Dirac spectrum in the (θ, φ) parameter space for which one has gapless plasmon modes, an example of which is shown in Fig. 2(a). In Fig. 2(g), the white regions correspond to polarizations for which the CP dispersion is gapped [as an example, see Fig. 2(b)]. Thus, changing the polarization allows one to *qualitatively* change the CP spectrum. This is further illustrated in Fig. 2(h), where we show the CP dispersion along the $K'\Gamma K$ direction [see Fig. 1(b)] for different angles θ of the polarization (in the figure, $\varphi = 0$). As one can see from Fig. 2(h), the two inequivalent Dirac points located at K and K' for $\theta = 0$ drift as one increases θ and they merge at $\mathbf{q} = 0$ for $\theta = \arcsin\sqrt{2/3}$, forming parabolic bands, to finally open a gap for $\theta > \arcsin\sqrt{2/3}$ (exemplified by $\theta = \pi/2$ in the figure).

A limitation on the experimental observability of the CP dispersion is plasmonic damping, which tends to blur the resonance frequencies. In order to estimate the feasibility of such experiments, we compare the bandwidth of the CP dispersion to the losses in individual nanoparticles. In the latter, two main sources of dissipation arise: (i) radiation damping with decay rate $\gamma_{\text{rad}} = 2r^3\omega_0^4/3c^3$ [35] (c is the speed of light), which dominates for larger nanoparticle sizes, and (ii) Landau damping with decay rate $\gamma_L = 3v_F g/4r$ [5,29,31] (v_F is the bulk Fermi velocity and g a constant of the order of 1), which dominates for

smaller sizes. Hence, there exists an optimal size $r_{opt} = (3v_F g c^3/8)^{1/4}/\omega_0$ for which the total damping $\gamma_{tot} = \gamma_{rad} + \gamma_L$ is minimal. For Ag nanoparticles, we find $r_{opt} = 8$ nm for which $\gamma_{tot} = 0.1$ eV/$\hbar$. With an interparticle distance $a = 3r_{opt}$ which maximizes the dipolar coupling between nanoparticles [12], we find that the bandwidth is of the order of $\Delta\omega = \omega_0^+ - \omega_0^- = \omega_0/9 = 0.6$ eV/$\hbar$ at the center of the Brillouin zone (for $\epsilon_m = 1$ and for the out-of-plane polarization). Thus, $\Delta\omega$ is sufficiently large when compared to γ_{tot} that the plasmon excitation is well defined and hence clearly measurable. Moreover, the appropriate use of active (gain-enhanced) media [36] might increase the observability of the CP dispersion.

A last comment is in order about the excitation of CPs by external photons, whose in-plane momentum must match the plasmonic one. In fact, the vicinity of the Dirac points typically lies outside the light cone. In order to overcome this momentum mismatch and observe the Dirac plasmons, one might add an extra periodic modulation of the lattice to allow grating coupling between the incident light and the desired collective modes [3]. Another alternative might be to use a nonlinear technique to overcome the momentum mismatch [37].

In conclusion, we demonstrated the strong analogies between the physical properties of electrons in graphene and those of collective plasmon modes in a 2D honeycomb lattice of metallic nanoparticles. Whereas the electronic states of graphene can be described by massless Dirac fermions, the CP eigenstates correspond to massless Dirac-like bosonic excitations. The spectrum of the latter can be fully tuned by the polarization of an external light field, opening exciting new possibilities for controlling the propagation of electromagnetic radiation with subwavelength lateral confinement in plasmonic metamaterials.

[1] M. Born and E. Wolf, *Principles of Optics* (Cambridge University Press, Cambridge, England, 2002).

[2] W. L. Barnes, A. Dereux, and T. W. Ebbesen, Nature (London) **424**, 824 (2003).

[3] S. A. Maier, *Plasmonics: Fundamentals and Applications* (Springer-Verlag, Berlin, 2007).

[4] T. Klar, M. Perner, S. Grosse, G. von Plessen, W. Spirkl, and J. Feldmann, Phys. Rev. Lett. **80**, 4249 (1998).

[5] U. Kreibig and M. Vollmer, *Optical Properties of Metal Clusters* (Springer-Verlag, Berlin, 1995).

[6] K. Kneipp, Y. Wang, H. Kneipp, L. T. Perelman, I. Itzkan, R. R. Dasari, and M. S. Feld, Phys. Rev. Lett. **78**, 1667 (1997).

[7] V. G. Veselago, Sov. Phys. Usp. **10**, 509 (1968); D. R. Smith, W. J. Padilla, D. C. Vier, S. C. Nemat-Nasser, and S. Schultz, Phys. Rev. Lett. **84**, 4184 (2000); R. A. Shelby, D. R. Smith, and S. Schultz, Science **292**, 77 (2001).

[8] J. B. Pendry, Phys. Rev. Lett. **85**, 3966 (2000); N. Fang, H. Lee, C. Sun, and X. Zhang, Science **308**, 534 (2005).

[9] U. Leonhardt, Science **312**, 1777 (2006); J. B. Pendry, D. Schurig, and D. R. Smith, Science **312**, 1780 (2006); D. Schurig, J. J. Mock, B. J. Justice, S. A. Cummer, J. B. Pendry, A. F. Starr, and D. R. Smith, Science **314**, 977 (2006).

[10] K. L. Tsakmakidis, A. D. Boardman, and O. Hess, Nature (London) **450**, 397 (2007).

[11] M. Quinten, A. Leitner, J. R. Krenn, and F. R. Aussenegg, Opt. Lett. **23**, 1331 (1998); J. R. Krenn, A. Dereux, J. C. Weeber, E. Bourillot, Y. Lacroute, J. P. Goudonnet, G. Schider, W. Gotschy, A. Leitner, F. R. Aussenegg, and C. Girard, Phys. Rev. Lett. **82**, 2590 (1999); S. A. Maier, M. L. Brongersma, P. G. Kik, and H. A. Atwater, Phys. Rev. B **65**, 193408 (2002); S. A. Maier, P. G. Kik, H. A. Atwater, S. Meltzer, E. Harel, B. E. Koel, and A. A. G. Requicha, Nat. Mater. **2**, 229 (2003).

[12] M. L. Brongersma, J. W. Hartman, and H. A. Atwater, Phys. Rev. B **62**, R16356 (2000); S. Y. Park and D. Stroud, Phys. Rev. B **69**, 125418 (2004).

[13] K. T. Carron, W. Fluhr, M. Meier, A. Wokaun, and H. W. Lehmann, J. Opt. Soc. Am. B **3**, 430 (1986); S. Zou, N. Janel, and G. C. Schatz, J. Chem. Phys. **120**, 10871 (2004).

[14] V. G. Kravets, F. Schedin, and A. N. Grigorenko, Phys. Rev. Lett. **101**, 087403 (2008); B. Auguié and W. L. Barnes, Phys. Rev. Lett. **101**, 143902 (2008); Y. Chu, E. Schonbrun, T. Yang, and K. B. Crozier, Appl. Phys. Lett. **93**, 181108 (2008).

[15] S. R. K. Rodriguez, G. Lozano, M. A. Verschuuren, R. Gomes, K. Lambert, B. De Geyter, A. Hassinen, D. Van Thourhout, Z. Hens, and J. Gómez Rivas, Appl. Phys. Lett. **100**, 111103 (2012).

[16] S. R. K. Rodriguez, A. Abass, B. Maes, O. T. A. Janssen, G. Vecchi, and J. Gómez Rivas, Phys. Rev. X **1**, 021019 (2011).

[17] H. A. Atwater and A. Polman, Nat. Mater. **9**, 205 (2010).

[18] K. S. Novoselov, A. K. Geim, S. V. Morozov, D. Jiang, Y. Zhang, S. V. Dubonos, I. V. Grigorieva, and A. A. Firsov, Science **306**, 666 (2004).

[19] P. R. Wallace, Phys. Rev. **71**, 622 (1947); A. H. Castro Neto, F. Guinea, N. M. R. Peres, K. S. Novoselov, and A. K. Geim, Rev. Mod. Phys. **81**, 109 (2009).

[20] K. S. Novoselov, A. K. Geim, S. M. Morozov, D. Jiang, M. I. Katsnelson, I. V. Grigorieva, S. V. Dubonos, and A. A. Firsov, Nature (London) **438**, 197 (2005); Y. Zhang, Y.-W. Tan, H. L. Stormer, and P. Kim, Nature (London) **438**, 201 (2005).

[21] V. V. Cheianov and V. I. Fal'ko, Phys. Rev. B **74**, 041403 (R) (2006).

[22] D. Han, Y. Lai, J. Zi, Z.-Q. Zhang, and C. T. Chan, Phys. Rev. Lett. **102**, 123904 (2009).

[23] F. D. M. Haldane and S. Raghu, Phys. Rev. Lett. **100**, 013904 (2008); O. Peleg, G. Bartal, B. Freedman, O. Manela, M. Segev, and D. N. Christodoulides, Phys. Rev. Lett. **98**, 103901 (2007); R. A. Sepkhanov, Y. B. Bazaliy,

and C. W. J. Beenakker, Phys. Rev. A **75**, 063813 (2007); S. R. Zandbergen and M. J. A. de Dood, Phys. Rev. Lett. **104**, 043903 (2010); J. Bravo-Abad, J. D. Joannopoulos, and M. Soljačić, Proc. Natl. Acad. Sci. U.S.A. **109**, 9761 (2012).

[24] D. Torrent and J. Sánchez-Dehesa, Phys. Rev. Lett. **108**, 174301 (2012).

[25] L. Tarruell, D. Greif, T. Uehlinger, G. Jotzu, and T. Esslinger, Nature (London) **483**, 302 (2012).

[26] This has been recently discussed numerically in the different context of classical waves in phononic and photonic crystals. See J. Mei, Y. Wu, C. T. Chan, and Z.-Q. Zhang, Phys. Rev. B **86**, 035141 (2012).

[27] L. M. Woods and G. D. Mahan, Phys. Rev. B **61**, 10 651 (2000); H. Suzuura and T. Ando, Phys. Rev. B **65**, 235412 (2002).

[28] I. M. Lifshitz, Sov. Phys. JETP **11**, 1130 (1960).

[29] A. Kawabata and R. Kubo, J. Phys. Soc. Jpn. **21**, 1765 (1966); C. Yannouleas and R. A. Broglia, Ann. Phys. (N.Y.) **217**, 105 (1992); R. A. Molina, D. Weinmann, and R. A. Jalabert, Phys. Rev. B **65**, 155427 (2002).

[30] L. G. Gerchikov, C. Guet, and A. N. Ipatov, Phys. Rev. A **66**, 053202 (2002).

[31] G. Weick, R. A. Molina, D. Weinmann, and R. A. Jalabert, Phys. Rev. B **72**, 115410 (2005); G. Weick, G.-L. Ingold, R. A. Jalabert, and D. Weinmann, Phys. Rev. B **74**, 165421

(2006); G. Weick, D. Weinmann, G.-L. Ingold, and R. A. Jalabert, Europhys. Lett. **78**, 27 002 (2007).

[32] C. Seoanez, G. Weick, R. A. Jalabert, and D. Weinmann, Eur. Phys. J. D **44**, 351 (2007); G. Weick, G.-L. Ingold, D. Weinmann, and R. A. Jalabert, Eur. Phys. J. D **44**, 359 (2007).

[33] Dipole-dipole interaction that decays algebraically with interparticle distance largely dominates here over other coupling mechanisms between the nanoparticles, such as tunneling of electrons [see K. J. Savage, M. M. Hawkeye, R. Esteban, A. G. Borisov, J. Aizpurua, and J. J. Baumberg, Nature (London) **491**, 574 (2012)]. At the frequencies of relevance for our analysis, electron ionization is irrelevant and each nanoparticle keeps a fixed number of electrons.

[34] See Supplemental Material at http://link.aps.org/supplemental/10.1103/PhysRevLett.110.106801 for the classical dynamics of CPs (including interactions beyond nearest neighbors) and for the condition for having gapless CPs.

[35] J. Crowell and R. H. Smith, Phys. Rev. **172**, 436 (1968).

[36] O. Hess, J. B. Pendry, S. A. Maier, R. F. Oulton, J. M. Hamm, and K. L. Tsakmakidis, Nat. Mater. **11**, 573 (2012).

[37] J. Renger, R. Quidant, N. van Hulst, S. Palomba, and L. Novotny, Phys. Rev. Lett. **103**, 266802 (2009).